RELIABILITY ANALYSIS OF A REINFORCED CONCRETE CONTAINMENT UNDER SEISMIC LOADING

H. Hwang (I)
N. C. Chokshi (II)
D. C. Jeng (II)
M. Reich (I)
Presenting Author: H. Hwang

SUMMARY

A reliability analysis method for nuclear containment structures has been developed by Brookhaven National Laboratory. This method incorporating finite element analysis and theory of random vibration, is able to evaluate the safety of structures under various static and dynamic loads. In this paper, the reliability analysis method is applied to a real reinforced concrete containment subjected to dead load and site-specific earthquake ground acceleration, which is assumed to be a Gaussian process with zero mean and Kanai-Tajimi spectrum. Furthermore, all seismic hazard is also included in the analysis. Finally, the reliability analysis results are presented.

INTRODUCTION

The safety of nuclear power plant structures is of primary concern to the regulatory agencies and the nuclear industry because of the serious socio-economic consequences that could result from structural failures. Recently, a probability-based reliability analysis method for containment structures has been developed by Brookhaven National Laboratory (BNL) (Ref. 1,2,3,4). An important feature of this methodology is the incorporation of finite element analysis and random vibration theory. By utilizing this method, it is possible to evaluate the safety of nuclear structures under various static and dynamic loads. In this paper, the results of the reliability analysis of a real reinforced concrete containment structure under dead load and earthquake ground acceleration are presented.

CONTAINMENT DESCRIPTION

The containment structure selected for the analysis is a real PWR containment in the U.S. Hence, the geometries and reinforcements of the containment are taken from the Final Safety Analysis Report (FSAR) and drawings. The containment structure consists of a vertical cylinder with a hemispherical dome on the top, and the cylinder-dome system is considered to

(I) Brookhaven National Laboratory, Upton, New York, USA

(II) Nuclear Regulatory Commission, Washington, D. C., USA

be fixed at the base. The containment structure and its dimensions are illustrated in Fig. 1. The containment wall is reinforced with hoop, meridional and diagonal rebars. The details of rebar arrangement for cylindrical portion and dome of the containment are tabulated in Tables 1 and 2, respectively.

In the present study, the material properties are taken to be the best estimated value. The variations of material properties will be included in the sensitivity studies in the future. The properties for the concrete and rebars are summarized as follows:

A) Concrete

The minimum compressive strength of concrete at 28 days is 3000 psi. However, the mean value is estimated to be 4896 psi from test data. The weight density of the concrete is taken to be 150 lb/ft^3. Young's modulus and Poisson's ratio are 3.1×10^6 psi and 0.2, respectively.

B) Reinforcing Bars

As can be seen from Tables 1 and 2, No. 18 rebars are the main reinforcement used in the containment structure. Hence, the statistics for No. 18 rebars is used to represent all other types of rebars. Young's modulus, E_s, and Poisson's ratio are taken to be 29.0×10^6 psi and 0.3, respectively. From the test data, the yield strength f_y is estimated to be 71.8 ksi.

FINITE ELEMENT ANALYSIS

In order to utilize the finite element analysis results in computing the limit state probabilities, the containment modelling should be made in such a way that the local coordinates of the elements have the same directions as those of the rebars. This is very easy to achieve in this study, since all the rebars are in the hoop and meridional directions.

The finite element utilized in the analysis is the shell element as described in the SAPV computer code. A three-dimensional finite element model as shown in Fig. 2 is used for the structural analysis of the containment. Also, a detailed cross-sectional view of the containment model is shown in Fig. 3. As can be seen from this figure, the containment is divided into 23 layers. Except the top layer of the dome, each layer has 24 elements such that the nodal points are taken every 15° in the circumferential direction. This discretization requires a total of 553 nodes and 540 elements.

For dynamic analysis of structures, modal analysis is employed. Hence, the dynamic characteristics of the structures are represented by the natural frequencies and associated mode shapes. Using the model described, the first 20 natural frequencies and corresponding modes are evaluated. It is important to choose the significantly participating modes which need to be included in the reliability analysis. In this study, only the first and second pairs of bending modes are chosen for the analysis.

PROBABILISTIC MODELS FOR LOADS

Various static and dynamic loads act on the containment structure during its lifetime. These loads may be caused by normal operating, environmental and accidental conditions. Since the loads intrinsically involve random and other uncertainties, an appropriate probabilistic model for each load must be established in order to perform reliability analysis. In this paper, only the dead load and earthquake ground acceleration are taken into consideration in the analysis.

Dead Load

The dead load primarily arises from the weights of the containment wall. It is noted that there are some uncertainties as to the actual magnitude of the dead load. For the purpose of this analysis, however, dead load is assumed to be deterministic and is equal to the design value, which is computed based on the weight density of reinforced concrete as 150 lb/ft^3.

Earthquake Ground Acceleration

The earthquake ground acceleration is assumed to act only along the global x (horizontal) direction. It is further assumed that the ground acceleration can be idealized as a segment of finite duration of a stationary Gaussian process with mean zero and Kanai-Tajimi spectrum;

$$S_{ggxx}(\omega) = S_o[1 + 4\xi_g^2(\omega/\omega_g)^2]/\{[1-(\omega/\omega_g)^2]^2 + 4\xi_g^2(\omega/\omega_g)^2\} \quad (1)$$

where the parameter S_o represents the intensity of the earthquake and ω_g and ξ_g are the dominant ground frequency and the ground damping ratio, respectively. The values of ω_g and ξ_g depend on the soil conditions of the chosen site. For the present study, $\omega_g = 8\pi$ rad/sec and $\xi_g = 0.6$ are used. Also, the mean duration μ_{dE} of the earthquake acceleration is assumed to be 15 seconds. The peak ground aceleration A_1, given an earthquake, is assumed to be $A_1 = p_g\sigma_g$ where p_g is the peak factor and is assumed to be 3.0 and σ_g is the standard deviation of the ground acceleration. By integrating Eq. 1 with respect to ω, σ_g is obtained as follows:

$$\sigma_g = \sqrt{\pi\omega_g[2\xi_g + 1/(2\xi_g)]} \quad \sqrt{S_o} \quad (2)$$

and

$$A_1 = \alpha_g \sqrt{So} \quad \text{with} \quad \alpha_g = p_g\sqrt{\pi\omega_g[2\xi_g + 1/(2\xi_g)]} \quad (3)$$

If the earthquake occurs in accordance with the Poisson law at a rate λ_E per year, it is easy to show that the probability distribution $F_A(a)$ of the annual peak ground acceleration A is related to the probability distribution $F_{A1}(a)$ of A_1 in the following fashion.

$$F_A(a) = \exp\{-\lambda_E[1 - F_{A1}(a)]\} \quad (4)$$

Therefore, if a_o indicates the minimum peak ground acceleration for any ground shaking to be considered an earthquake, $F_{A1}(a_o) = 0$ and hence $\lambda_E = - \ln F_A(a_o)$. Assuming that $F_A(a)$ is of the extreme distribution of Type II, $F_A(a) = \exp[-(a/u)^{-\alpha}]$ with $\alpha = 3.14$ and $u = 0.0135$, one finally obtains

$$F_{A1}(a) = 1 - (a/a_o)^{-\alpha} \qquad a \geqslant a_o \tag{5}$$

Under these conditions, one finds that $\lambda_E = 1.64 \times 10^{-2}$/year provided that $a_o = 0.05g$. Combining Eqs. (3) and (5) and writing Z for $\sqrt{S_o}$, one further obtains the probability distribution of Z as follows:

$$F_Z(z) = 1 - (\alpha_g z/a_o)^{-\alpha} \quad z \geqslant a_o/\alpha_g \tag{6}$$

The information about the maximum earthquake ground acceleration, a_{max}, which represents the largest earthquake possible to occur at a particular site is needed in order to determine the limit state probability. In this study, a_{max} is chosen to be equal to 0.71g.

LIMIT STATE FOR CONTAINMENT

In this paper, the limit state is defined according to the ultimate strength theory of the reinforced concrete. For flexural failure of a element, the limit state is reached when a maximum compressive strain at the extreme fiber of the cross-section is equal to 0.003, while the yielding of rebars is permitted. Based on the above definition of the limit state and the theory of reinforced concrete, for each cross-section of a finite element, a limit state surface can be constructed in terms of the membrane stress τ and bending moment m, which is taken about the center of the cross-section (Ref. 5). A typical limit state surface is shown in Fig. 4. In this figure, point "a" is determined from a stress state of uniform compression and point "e" from uniform tension. Points "c" and "c'" are so-called "balanced point", at which a concrete compression strain of 0.003 and a steel tension strain of f_y/E_s are reached simultaneously. Furthermore, lines abc and ab'c' in Fig. 4 represent compression failure. Lines cde and c'd'e represent tension failure.

LIMIT STATE PROBABILILTY

Analytically, the eight straight lines of the limit state surface as shown in Fig. 4 are expressed as follows:

$$R_j - [A_j]^T [\tau^{(e)}] = 0 \qquad j=1,2,\ldots 8 \tag{7}$$

where $[\tau^{(e)}]$ is the element stress vector, and R_j and $[A_j]$ are constants and constant vectors, respectively. In this paper, the stress vector, $[\tau^{(e)}]$, consists of two vectors; $[\tau^{(e)}]_o$, and $[\tau^{(e)}]_d$. The vector $[\tau^{(e)}]_o$ is the stress vector due to dead load and is time-invariant and deterministic based on the dead load assumption. The vector $[\tau^{(e)}]_d$ is stress vector due to the earthquake acceleration and it can be computed as (Refs. 1, 2).

$$[\tau^{(e)}]_d = Z[c^{(e)}][v_o] \text{ with } [c^{(e)}] = [B^{(e)}] [\phi^{(e)}] [L_q] \tag{8}$$

In this expression, $[B^{(e)}]$ and $[\phi^{(e)}]$ are such that $[\tau^{(e)}] = [B^{(e)}]\ [u^{(e)}]$ with $[u^{(e)}]$ being the element nodal displacement vector and $[u^{(e)}] = [\phi^{(e)}]\ [q]$ with $[q]$ being the generalized coordinate vector, respectively. The vector $[v_o]$ is obtained from a linear transformation $[q_o] = [L_q]\ [v_o]$ such that the covariance matrix $[V_{v_o v_o}]$ of $[v_o(t)]$ becomes $[I_m]$ = mxm identity matrix (m=number of modes considered). The vector $[q_o]$ is the generalized coordinate vector when $Z = \sqrt{S_o} = 1\sqrt{in^2/sec^3}$. Thus, $[\tau^{(e)}]$ has the following expression:

$$[\tau^{(e)}] = [\tau^{(e)}]_o + Z\ [c^{(e)}]\ [v_o] \tag{9}$$

Substitating Eq. (9) into Eq. (7), one obtains

$$\gamma_j^{(e)} - Z[n_j^{(e)}]^T\ [v_o] = 0 \tag{10}$$

where

$$[n_j^{(e)}] = [\bar{A}_j^{(e)}]/|\bar{A}_j^{(e)}| \quad \text{with} \quad [\bar{A}_j^{(e)}]^T = [A_j]^T[c^{(e)}]$$

and

$$\gamma_j^{(e)} = (R_j - [A_j]^T\ [\tau^{(e)}]_o)/|\bar{A}_j^{(e)}|$$

Let $X_{mj}^{(e)}$ be max $|[n_j^{(e)}]^T\ [v_o]|$ in $0 \leq t \leq \mu_{DE}$ and the probability distribution of $X_{mj}^{(e)}$ is derived in Ref. 2.

The conditional limit state probability with respect to line j, $P_j\ (e)$, is obtained as

$$P_j^{(e)} = \Pr\ [\gamma_j^{(e)} - ZX_{mj}^{(e)} \leq 0\ ] \tag{11}$$

Assuming the containment will not fail under dead load alone, then $\gamma_j^{(e)}$ is positive and $P_j^{(e)}$ can be expressed as follows: (Refs. 1, 2)

$$P_j^{(e)} = \int_{Z_{min}}^{Z_{max}} \nu_{jo}^{(e)} \mu_{dE}\ \exp[1/2(\gamma_j^{(e)}/z)^2]\ f_Z(z)dz \tag{12}$$

Furthermore, the conditional limit state probability of the element, P(e), will be bounded as follows:

$$\max P_j^{(e)} \leq p(e) \leq \sum_{j=1}^{8} P_j^{(e)} \tag{13}$$

Finally, the unconditional limit state probability, P_f, during the lifetime T years is approximated as

$$P_f = T\,\lambda_E\ P(e) \tag{14}$$

RELIABILITY ANALYSIS RESULTS

On the basis of the finite element model, limit state, loading conditions and reliability analysis method described in the preceding sections, a reliability analysis of the containment under the combination of dead load and earthquake ground acceleration has been carried out. The limit state is reached as the tensile yielding of meridional rebars in the critical elements 6, 7, 18 and 19. These critical elements are located at the first layer and adjacent to global x-axis. The locations of the critical elements and the manner in which the limit state is reached are obviously consistent with the structural and loading symmetry with respect to the x-axis. The lower and upper bounds of the conditional limit state probability $P^{(D+E)}$ are found to be very close and equal to 1.02×10^{-8}. Finally, the unconditional limit state probability during the lifetime of 40 years is 6.72×10^{-9}.

REFERENCES

1. Hwang, H., Shinozuka, M., Brown, P. and Reich, M., "Reliability Assessment of Reinforced Concrete Containment Structures", BNL-NUREG-51661, NUREG/CR-3227, February, 1983.

2. Kako, T., Shinozuka, M., Hwang, H. and Reich, M., "FEM-Based Random Vibration Analysis of Nuclear Structures Under Seismic Loading", SMiRT-7 Conference, Paper K 7/2, Chicago, IL, August 22-26, 1983.

3. Shinozuka, M., Kako, T., Hwang, H. and Reich, M., "Development of a Reliability Analysis Method for Category I Structures", SMiRT-7 Conference, Paper M 5/3, Chicago, IL, August 22-26, 1983.

4. Shinozuka, M., Kako, T., Hwang, H., Brown, P. and Reich, M., "Estimation of Structural Reliability Under Combined Loads", SMiRT-7 Conference, Paper M 2/3, Chicago, IL, August 22-26, 1983.

5. Chang, M., Brown, P., Kako, T., Hwang, H., "Structural Modeling and Limit State Identification for Reliability Analysis of RC Containment Structures:, SMiRT-7 Conference, Paper M3/2, Chicago, IL, August 22-26, 1983.

ACKNOWLEDGEMENTS

The authors wish to express their appreciation to Professor M. Shinozuka, Columbia University and Mr. H. Ashar of the Nuclear Regulatory Commission for their guidance during various phases of this study.

Thanks are due to Mr. J. Kawakami for numerical computation and to Ms. J. DePass for the typing of this paper.

NOTICE

The views expressed in this paper are those of the authors. The technical contents of this paper have neither been approved nor disapproved by the United States Nuclear Regulatory Commission.

Table 1 Cylinder Reinforcement

Elevation	Hoop	Meridional		Diagonal
		Primary	Secondary	
0 to 25'-0"	2#18 @ 14 in	1#18 @ 12 in	1#18 @ 12 in	1#18 @ 30 in
25'-0" to 45'-5"	"	"	1#11 @ 12 in	"
45'-5" to 50"-3"	"	"	2#11 @ 36 in	"
50'-3" to 54'-10"	"	"	1#11 @ 36 in	"
54'-10" to 110'-6"	"	"		"
110'-6" to 148'-0"	"	"		1#18 @ 60 in 1#14 @ 60 in +

Table 2 Dome Reinforcement

Angle From Spring Line (Degrees)	Hoop	Meridional	Diagonal
0°-9.5°	1#14 {@ 8 1/4" outside @ 8.0" inside}	1#18 @ 0.796°	1#18+1#14 @ 4° (horiz. dist.)
9.5°-18.5°	1#14 @ 8.0 in	"	"
18.5°-35°	"	"	1#11 @ 2° (horiz. dist.)
35°-55°	"	"	
55°-60°	1#14 @ 9.0 in	"	
60°-75°	"	1#18 @ 1.593°	
75°-83°	"	1#18 @ 3.186°	
83°-86°	"	1#18 @ 6.37°	
86°-90°	"	1#18 @ 12.74°	

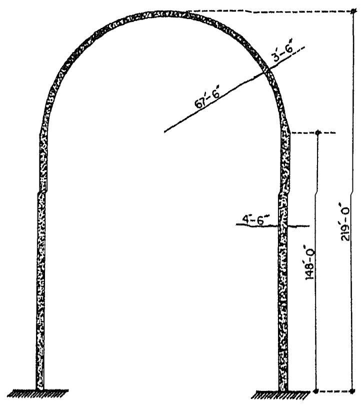

Fig. 1 Reinforced Concrete Containment Structure.

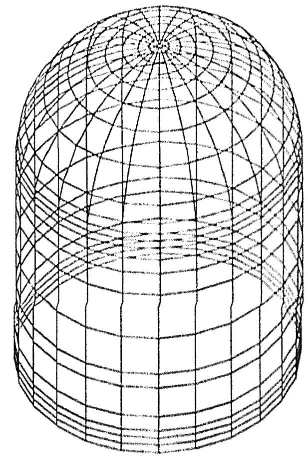

Fig. 2 Three-Dimensional Model for Containment.

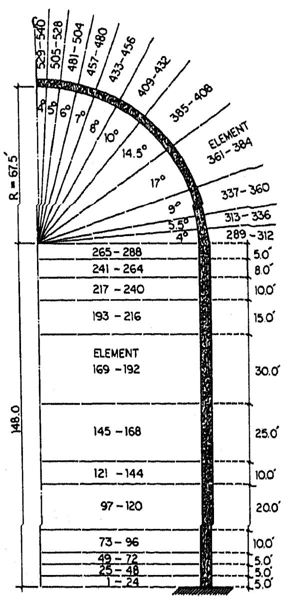

Fig. 3 Cross Section of Containment Model.

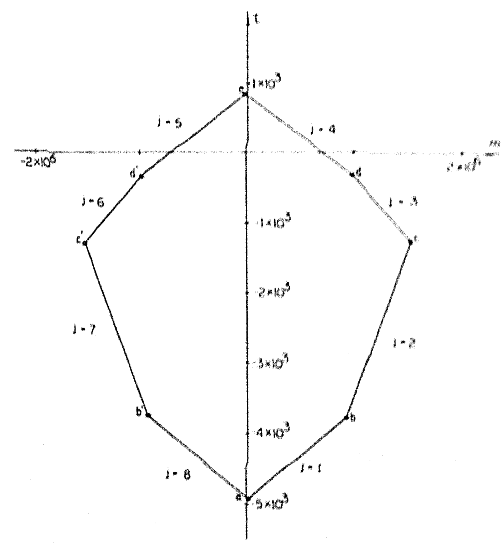

Fig. 4 Limit State Surface.